Available online at www.sciencedirect.com

ScienceDirect

Geochimica et Cosmochimica Acta 141 (2014) 83–96

Geochimica et Cosmochimica Acta

www.elsevier.com/locate/gca

Extending the analytical window for water-soluble organic matter in sediments by aqueous Soxhlet extraction

Frauke Schmidt [a,*], Boris P. Koch [a,b,c], Matthias Witt [d], Kai-Uwe Hinrichs [a]

[a] *MARUM – Center for Marine Environmental Sciences, University of Bremen, Leobener Straße, D-28359 Bremen, Germany*
[b] *Alfred-Wegener-Institut Helmholtz-Zentrum für Polar- und Meeresforschung, Am Handelshafen 12, D-27570 Bremerhaven, Germany*
[c] *University of Applied Sciences, An der Karlstadt 8, D-27568 Bremerhaven, Germany*
[d] *Bruker Daltonik GmbH, Fahrenheitstraße 4, 28359 Bremen, Germany*

Received 9 July 2013; accepted in revised form 12 June 2014; Available online 24 June 2014

Abstract

Dissolved organic matter (DOM) in marine sediments is a complex mixture of thousands of individual constituents that participate in biogeochemical reactions and serve as substrates for benthic microbes. Knowledge of the molecular composition of DOM is a prerequisite for a comprehensive understanding of the biogeochemical processes in sediments. In this study, interstitial water DOM was extracted with Rhizon samplers from a sediment core from the Black Sea and compared to the corresponding water-extractable organic matter fraction (<0.4 μm) obtained by Soxhlet extraction, which mobilizes labile particulate organic matter and DOM. After solid phase extraction (SPE) of DOM, samples were analyzed for the molecular composition by Fourier Transform Ion-Cyclotron Resonance Mass Spectrometry (FT-ICR MS) with electrospray ionization in negative ion mode. The average SPE extraction yield of the dissolved organic carbon (DOC) in interstitial water was 63%, whereas less than 30% of the DOC in Soxhlet-extracted organic matter was recovered. Nevertheless, Soxhlet extraction yielded up to 4.35% of the total sedimentary organic carbon, which is more than 30-times the organic carbon content of the interstitial water. While interstitial water DOM consisted primarily of carbon-, hydrogen- and oxygen-bearing compounds, Soxhlet extracts yielded more complex FT-ICR mass spectra with more peaks and higher abundances of nitrogen- and sulfur-bearing compounds. The molecular composition of both sample types was affected by the geochemical conditions in the sediment; elevated concentrations of HS^- promoted the early diagenetic sulfurization of organic matter. The Soxhlet extracts from shallow sediment contained specific three- and four-nitrogen-bearing molecular formulas that were also detected in bacterial cell extracts and presumably represent proteinaceous molecules. These compounds decreased with increasing sediment depth while one- and two-nitrogen-bearing molecules increased, resulting in a higher similarity of both sample types in the deep sediment. In summary, Soxhlet extraction of sediments accessed a larger and more complex pool of organic matter than present in interstitial water DOM.

1. INTRODUCTION

Organic matter in marine sediments is a major reservoir of reduced carbon on Earth and an important player in the global carbon and nutrient cycle (Hedges and Keil, 1995). It is a highly complex and diverse organic mixture derived from marine and from terrestrial biological sources. Most of this organic matter is chemically altered during transport through the water column and sedimentation. Labile compounds are remineralized or modified and recalcitrant compounds accumulate in the sediment (Wakeham et al., 1997; Veuger et al., 2012). The buried organic matter reservoir is

* Corresponding author. Tel.: +49 421 21865705; fax: +49 421 21865715.
E-mail address: frauke.schmidt@uni-bremen.de (F. Schmidt).

http://dx.doi.org/10.1016/j.gca.2014.06.009
0016-7037/

an important energy supply for microbes in subsurface sediments (Whitman et al., 1998; Parkes et al., 2000; D'Hondt et al., 2004; Biddle et al., 2006; Webster et al., 2006), which play an important role in biogeochemical element cycles (Kvenvolden, 1993; D'Hondt et al., 2002). The preservation mechanisms and availability of organic matter to microbes depends on molecular properties such as composition, size and structure (Weiss et al., 1991; Arnosti et al., 2011). For a better understanding of the biogeochemical processes in the sediment, knowledge of the molecular organic matter composition is a prerequisite, particularly of dissolved organic matter (DOM) which accumulates in interstitial water in the sediment as a result of particulate organic matter depolymerization. In the last decade, ultrahigh-resolution Fourier Transform Ion-Cyclotron Resonance Mass Spectrometry (FT-ICR MS) has extended the analytical window for organic matter characterization due to its capacity for resolving thousands of constituents with individual elemental compositions in complex DOM mixtures. FT-ICR MS provided insights into the sources of DOM in various environments (Kim et al., 2004; Koch et al., 2005; Dittmar and Koch, 2006; Hertkorn et al., 2006; Tremblay et al., 2007; Reemtsma et al., 2008; Schmidt et al., 2009; Bhatia et al., 2010; D'Andrilli et al., 2010; Lechtenfeld et al., 2013; Roth et al., 2013) and it revealed transformation of DOM related to microbial processes (Kim et al., 2006; Longnecker and Kujawinski, 2011; Schmidt et al., 2011), fungal degradation (Grinhut et al., 2011), and photochemical alteration (Kujawinski et al., 2004; Gonsior et al., 2009).

This study exploits FT-ICR MS for the characterization of interstitial water DOM (IW-DOM) and the water extractable sedimentary organic matter fraction of a 8.75-m-long sediment core from the Black Sea. IW-DOM was extracted with Rhizon samplers (Seeberg-Elverfeldt et al., 2005) from a sediment depth of down to 6 m below seafloor and compared to the organic matter (fraction <0.4 μM) that is extractable with hot water in a Soxhlet apparatus (water extractable organic matter WE-OM). Hot water extraction of organic matter has been previously applied to determine the labile organic matter fraction in soils (e.g., Sparling et al., 1998; Ghani et al., 2003; Gregorich et al., 2003; Bu et al., 2010; Xing et al., 2010; Sarkhot et al., 2011). However, to our knowledge, it has never been utilized for the molecular characterization of organic matter in marine sediments. WE-OM is one potential source for IW-DOM. We assume that not only the IW-DOM fraction is accessible to microbial attack but also the organic matter that is attached more tightly to the sediment matrix, e.g., by sorption to mineral surfaces or binding in complexes and polymeric aggregates (Keil et al., 1994; Arnarson and Keil, 2005). Conceptually, we expect this organic matter fraction to be relatively concentrated in WE-OM of marine sediments as it has been shown for soils before (Curtin et al., 2011). Hence, analysis of this pool will expand the information regarding microbially relevant organic constituents in marine sediments. Furthermore, aqueous Soxhlet extraction is a promising approach to obtain information about the DOM pool when the interstitial water volume is not sufficient for FT-ICR MS analysis, e.g., in clay-rich sediments or consolidated sediment from great depths. It has been successfully applied for the extraction of low-molecular-weight organic acids from coal, sand- and mudstones as potential feedstock for the deep biosphere (Vieth et al., 2008).

The main goals of this study were to examine (i) the portion of "dissolved" organic matter that can be obtained by Rhizon *vs.* Soxhlet extraction; (ii) the changes in the organic matter composition related to burial depth, geochemical conditions, lithology, and provenance of the sediment; (iii) the differences in molecular composition between IW-DOM and WE-OM in corresponding samples.

2. MATERIAL AND METHODS

2.1. Sampling

Samples were taken during FS Meteor Expedition M84-1 at GeoB Station 15105 in February 2011 in the Black Sea. A gravity core and a multicore were retrieved from 1266 m water depth at latitude 41°31′71 N and longitude 30°53′07 E. Interstitial water and sediment samples were taken from one depth of the multicore (10–12 cm) and three different depths of the gravity core (147–162, 420–435, 596–613 cm) representing different stratigraphic units. Interstitial water was sampled with Rhizons (Eijkelkamp, pore size 0.1 μm). Rhizon samplers were connected to 20-ml syringes and interstitial water was sampled by applying vacuum (duration of sampling: 4–6 h). Aliquots of the interstitial water were taken for dissolved organic carbon (DOC) and total dissolved nitrogen (TDN) analyses and stored at −20 °C in the dark. The main fraction of the interstitial water was stored under N_2 atmosphere at +4 °C in the dark until further processing on board. Sediment was sampled in selected intervals of the open core and stored at −20 °C in the dark until further processing in the home laboratory.

2.2. Soxhlet extraction of sediments

Sediments were homogenized and cryogenically ground in a cryomill (Retsch, Cryomill, Haan) cooled with liquid nitrogen. Subsequently, around 25 g of the wet sediment (including interstitial water DOM) was weighted into precombusted glass fiber thimbles (30 × 100 mm, Whatman) which were extracted before with distilled ultrapure water for 48 h to remove potential contaminants. 200 ml of distilled, deionized water was added to the round-bottom flask of the Soxhlet extraction unit together with boiling chips (PTFE, Roth), and the Soxhlet system was flushed with argon through a valve in round-bottom flask to create an inert atmosphere. Afterwards, the system was closed with a gas balloon that was attached to the top of the condenser unit. Extraction was carried out for 48 h in the dark to avoid photochemical reactions. After extraction, the extract solution was filtered through a GF-5 filter (Mackerey-Nagel, pore size 0.4 μm) in N_2 atmosphere to avoid oxidation reactions and stored at +4 °C until further preparation. Any possible effects of the different pore sizes used for Soxhlet extracts and IW-DOM on the molecular composition can be neglected due to our analytical mass

window of <1000 Da, which corresponds to molecules considerably smaller than the rhizon pore size of 0.1 μm.

2.3. Preparation and extraction of *Escherichia coli*

Escherichia coli (DSM No. 11250, DSMZ) was cultivated in 100 ml sterile medium consisting of 500 mg peptone (Alfa Aesar), 500 mg tryptone (Fluka), 500 mg sodium chloride (VWR), 500 mg yeast extract (Alfa Aesar) at pH 7 and 28 °C for 40 h. The culture was split into two samples. After centrifugation (4000 rpm, for 15 min) the supernatants were decanted and the cells were washed 3-times with a sodium chloride solution (5‰ NaCl). Subsamples were taken for cell enumeration. Afterwards each *E. coli* sample split was added to 15 g of combusted quartz sand in pre-combusted and pre-extracted glass fiber thimbles. Soxhlet extraction of *E. coli* samples was carried out similarly to the sediment samples (see Section 2.2) and afterwards the extracts were filtered through GF-5 filters. Cells were enumerated by epifluorescence microscopy of 2% formaldehyde-fixed samples using SYBR green I staining solution as described by Lunau et al. (2005).

2.4. DOM extraction

Between 22 and 37 ml of the interstitial water were prepared for FT-ICR MS analyses on board under N_2 atmosphere in a glove bag to avoid possible oxidation of the DOM. All reagents were degassed by N_2 treatment with precombusted Pasteur pipettes before use. Soxhlet extracts from sediments and *E. coli* were prepared in the home laboratory under similar conditions. First, samples were acidified to pH 2 with hydrochloric acid (suprapur, Merck) and concentrated by solid phase extraction (SPE) on precleaned Bond Elut-PPL cartridges (200 mg sorbent, Agilent Inc.) according to the protocol by Dittmar et al. (2008). After adsorption, salts were removed by rinsing the cartridge with 6 ml ultrapure water (pH 2) and DOM was eluted with 0.5 ml (for interstitial waters) and 1 ml methanol (LiChrosolv, Merck) for the Soxhlet extracts. A procedural blank was performed to check for possible contaminations during sample extraction. SPE extracts were stored in precombusted HPLC vials under N_2 atmosphere at −20 °C in the dark until FT-ICR MS analyses.

2.5. Dissolved organic carbon and total dissolved nitrogen

DOC and TDN concentrations were analyzed in the interstitial waters, in the water-soluble, filtrated fraction derived from Soxhlet extraction, and in the SPE extracts. Prior to analyses of the SPE extracts, the solvent was removed from aliquots of the extracts under a stream of nitrogen and the DOM was re-dissolved in 6 ml ultrapure water. Measurements were carried out by high-temperature catalytic oxidation using a Shimadzu TOC/TN analyzer equipped with an infrared and a chemiluminescence detector (oxygen flow: 0.6 l min^{-1}). The samples were acidified with 0.12 ml HCl (2 M) in the autosampler and purged with oxygen to remove inorganic carbon. Afterwards, the sample was directly injected onto the catalyst and heated to 680 °C. Final DOC concentrations were average values of triplicate measurements. The DOC and TDN concentration of the procedural blank was below limit of determination indicating that SPE did not introduce any additional DOC or TDN. Solid phase extraction efficiencies for all samples were calculated from DOC concentrations in the original sample and aliquots of the SPE extracts. The total water soluble organic carbon (OC) was calculated as follows: (1) DOC concentrations of WE-OM and IW-DOM were normalized to g wet sediment, considering the amount of water and sediment that was used for Soxhlet extractions and the volume of interstitial water obtained from 1 g sediment by Rhizon sampling (Table S1 Appendix A); (2) concentrations expressed in μmol/g sediment were transformed into μg OC/g sediment, (3) μg OC/g sediment was normalized to the sedimentary TOC at each sample depth (Table 1).

2.6. Fourier transform ion-cyclotron resonance mass spectrometry

DOM extracts were diluted with methanol:water (1:1, v/v) and analyzed in a concentration of 750 nM DOC/μL. Samples were ionized with electrospray ionization (ESI, Apollo II electrospray source, Bruker Daltonik GmbH, Bremen, Germany) in negative ion mode at an infusion flow rate of 2 μl min^{-1} on a Bruker SolariX FT-ICR MS (Bruker Daltonik GmbH, Bremen, Germany) equipped with a 12 T refrigerated actively shielded superconducting magnet (Bruker Biospin, Wissembourg, France). Initially, mass spectra were calibrated externally with arginine clusters in negative ion mode using a linear calibration. Ion accumulation time was set to 0.05 s for IW-DOM and 0.03 s for WE-OM due to the higher complexity of WE-OM. 300 scans were added to one mass spectrum ranging from *m/z* 150 to 3000. *E. coli* samples were analyzed with an ion accumulation time of 0.24 s and 500 scans were added to one mass spectrum. Mass spectra were acquired with 4 MW data points resulting in a resolving power of 480,000 at *m/z* 400. Subsequently, mass spectra were recalibrated internally with compounds that were repeatedly identified in marine interstitial water DOM samples ($C_{13}H_{16}O_5$: *m/z* 247.06120, $C_{15}H_{21}O_6$: *m/z* 297.13436, $C_{16}H_{23}O_7$: *m/z* 327.14493, $C_{18}H_{25}O_8$: *m/z* 369.15549, $C_{19}H_{25}O_9$: *m/z* 397.15041, $C_{21}H_{27}O_{10}$: *m/z* 439.16097, $C_{23}H_{31}O_{11}$: *m/z* 483.18719, $C_{28}H_{39}O_{11}$: *m/z* 551.24979, $C_{29}H_{39}O_{13}$: *m/z* 595.23962). The root mean square error of the internal calibration was below 0.135 ppm for the interstitial waters and below 0.100 ppm for the Soxhlet extracts and 0.055 ppm for *E. coli* extracts. Molecular formulas were calculated by considering the following elements $^{1}H_{0–120}$, $^{12}C_{0–50}$, $^{13}C_{0–1}$, $^{16}O_{0–35}$, $^{14}N_{0–4}$, $^{32}S_{0–2}$, $^{34}S_{0–1}$, $^{31}P_{0–2}$ in a *m/z* range of 150–650. Formulas were restricted to a molecular element ratio of O/C $\leqslant$ 1.2 and to integer double bond equivalent (DBE) values. A mass tolerance of ±0.5 ppm was considered as a valid formula. For the final dataset we focused on ions with an average S/N $\geqslant$ 10 corresponding to a relative intensity $\geqslant$3% (normalized to the highest sample peak in each spectra) in a *m/z* range of 180–600, using the following restrictions with respect to the molecular composition: $^{1}H_{0–120}$, $^{12}C_{0–50}$, $^{16}O_{0–35}$, $^{14}N_{0–4}$, $^{32}S_{0–2}$, $^{31}P_{0–2}$.

Table 1
Total organic matter and sediment properties of samples from core GeoB 15105 from the Black Sea.

Depth (cm)	TOC (%)	$\delta^{13}C_{TOC}$ (‰)	TN (%)	$\delta^{15}N$ (‰)	TOC/TN	Lithology	Age (ka BP)
10–12	1.69	−24.6	0.18	4.1	11.0	Laminated coccolith ooze	
147–162	1.43	−24.6	0.13	2.8	12.8	Laminated coccolith ooze	3.55–3.58
420–435	1.23	−26.1	0.14	3.4	10.3	Limnic clay with carbonate clasts	>8
596–613	1.12	−26.3	0.08	4.4	16.3	Dark banded sulfide rich clayey mud	

Multiple formulas were filtered with the homologous series/building block approach and isotope check (Koch et al., 2007) yielding up to 9,749 unequivocal formulas per sample and <10 peaks with double assignments per sample. Potentially anthropogenic surfactants that were listed in a surfactant database (http://www.terrabase-Inc.com) were removed from the final data set. The spectra of the Soxhlet extracts contained also peaks above the intensity threshold of 3% in the range of 150–180 Da and 600–650 Da that were not included in this study to allow a comparison of both sample types in statistical analysis.

For multivariate statistical analysis a principal component analyses (PCA) was performed on normalized peak magnitudes using the software R.

2.7. Total organic carbon, total nitrogen, and stable carbon and nitrogen isotopes

Total organic carbon (TOC) content, total nitrogen (TN) content, and the stable carbon and nitrogen isotopic compositions were analyzed from the freeze-dried homogenized sediment. Prior to analysis, 3 g of the sediment was decalcified by the addition of 10% HCl and afterwards washed with ultrapure water. Between 10 and 30 mg of the dried sediment was weighed into tin capsules and analyzed for TOC and TN as well as their stable isotopes on a Thermo Scientific Flash 2000 elemental analyzer connected to a Thermo Delta V Plus IRMS. TOC, TN and stable isotope values are mean values of analysis of duplicate samples. TOC and TN values are given in % per g dry sediment and isotopic values are quoted in the $\delta^{13}C$ and $\delta^{15}N$ notation in ‰ relative to the Vienna Pee Dee Belemnite (V-PDB) standard and atmospheric N, respectively. Standard deviation for isotope measurements was below 0.1‰ for C and below 0.3‰ for N as determined from repeated analysis of a reference sample.

3. RESULTS

3.1. Sediment and bulk organic matter properties

The samples from four sediment depths represented different types of sediment, depositional regimes, and ages (Table 1). All sediments were clay-rich and the upper two samples (10–12, 147–162 cm) consisted of finely laminated coccolith ooze of marine Unit I in the Black Sea (Degens and Ross, 1972). 147–162 cm contained a volcanic ash layer which most likely derived from the Minoan eruption of Santorini, and therefore dates to 3.55–3.58 ka BP (Friedrich et al., 2006; Kwiecien and Haug, 2008). The sample from 420 to 435 cm consisted of clay with sand to silt-sized carbonate clasts and was deposited when the Black Sea was isolated from the Mediterranean (Black Sea Unit III; age > 8 ka BP) (Bahr et al., 2006; Kwiecien and Haug, 2008). The deepest sample (596–613 cm) represented a dark banded sulfide-rich clayey mud from Unit III. TOC and TN concentrations in the sediment samples ranged from 1.69% to 1.12% and 0.18% to 0.08%, respectively (Table 1). $\delta^{13}C_{TOC}$ decreased with increasing sediment depth from −24.6‰ to ^{13}C-depleted values of −26.3‰. $\delta^{15}N$ showed the lowest value of 2.8‰ in 147–162 cm depth and the highest value of 4.4‰ in 596–613 cm depth.

TOC and TN concentrations decreased with sediment depth (Table 1), whereas DOC and TDN was higher in the deeper sediment (Table 2). In order to compare the DOC concentration of the interstitial water and the Soxhlet extract, we normalized the measured DOC concentration to grams of wet sediment. Normalized carbon concentrations in the Soxhlet extracts were up to 50 times higher than in the corresponding interstitial water and ranged between 40.03 and 49.04 μM C/g sediment (including interstitial water DOC) compared to 0.73 to 1.77 μM C/g sediment in IW-DOM (Table 2).

3.2. Extraction efficiency for IW-DOM and WE-OM

The extraction efficiency for IW-DOM was in the range of 39–87% and showed an increase with depth. In contrast, extraction efficiency for WE-OM was considerably lower; only 11–28% of the DOC was recovered after SPE and the extraction efficiency was lowest in the deepest sample (Table 2). However, even with these relatively low extraction efficiencies, a substantially larger total amount of the WE-DOM pool was recovered (11.21 μmol C/g sed *vs.* 0.27 μmol C/g sed in 10–12 cm depth, Table 2) and at 6 m sediment depth, the WE-OM was at least 4-times larger than the IW-DOM pool (4.48 μmol C/g sed *vs.* 1.06 μmol C/g sed).

From the total pool of nitrogen compounds, SPE only extracts dissolved organic nitrogen (DON). Inorganic N compounds such as ammonium and nitrate are not retained on the column. Portions of solid phase-extractable DON (SPE-DON) relative to TDN ranged between 3% (10–12 cm) and 8% (420 cm) for IW-DOM and between 38% (147–162 cm) and 45% (596–613 cm) for WE-OM (Table 2). Absolute SPE-DON concentrations in IW-DOM increased from 24 μM in 10–12 cm depth to a maximum of 137 μM DON in 420–435 cm, whereas SPE-DON concentrations in WE-OM decreased with depth from 119 μM in 10–12 cm depth to 51 μM DON in 596–613 cm depth.

Table 2
Bulk composition of DOM and solid phase extraction efficiencies (extr. eff.) in interstitial water and Soxhlet extracts from core GeoB 15105 and from *E. coli* (two replicates, each 40 mg). The concentration of solid-phase-extractable dissolved organic nitrogen (SPE-DON) is compared to its percentage of total dissolved nitrogen (TDN; numbers in brackets). Organic carbon (OC) concentration of interstitial water and Soxhlet extracts were normalized to sediment weight to calculate their relative contributions to the total OC in the sediments.

Depth (cm)	DOC_{IW} (μM)	TDN_{IW} (μM)	$SPE\text{-}DON_{IW}$ (μM)	DOC_{WE} (μM)	TDN_{WE} (μM)	$SPE\text{-}DON_{WE}$ (μM)	DOC extr. eff. (%)		OC (μmol C/g sed)		IW-OC (%)	WE-OC (%)
							IW	WE	in IW	in WE		
10–12	1053	808	24 (3%)	4109	289	119 (41%)	39	28	0.73	40.03	0.05	2.85
147–162	3335	2155	86 (4%)	5787	227	86 (38%)	47	17	1.77	49.04	0.15	4.11
420–435	2992	1715	137 (8%)	4761	189	79 (42%)	77	20	1.44	43.07	0.14	4.19
596–613	2303	1516	91 (6%)	5788	114	51 (45%)	87	11	1.22	40.70	0.13	4.35
E. coli 1				1041	394	56 (19%)		56				
E. coli 2				1040	300	51 (17%)		58				

3.3. FT-ICR MS analyses

3.3.1. Molecular variations in IW-DOM from different sediment depths

FT-ICR-MS provided exact molecular masses of singly charged ions which allowed to calculate molecular formulas. It is important to note that each formula can represent a plethora of different molecules with different molecular conformations (Hertkorn et al., 2008). In the following, for the ease of readability, we generally refer to a calculated molecular formula as a "compound" or "constituent".

Although ESI-FT-ICR MS is not quantitative, samples can be compared semi-quantitatively based on the relative intensity of their constituents in the spectra (here normalized to the base peak of each sample), if analyzed under similar conditions and instrument settings (Kido Soule et al., 2010; Sleighter et al., 2012). Therefore, prior to FT-ICR MS analyses all samples were diluted to a similar DOC concentration and analyzed in sequence on one day using identical instrument settings to allow a comparison of the spectra. Between 3244 and 5790 molecular formulas were identified in a m/z range of 180–600 Da in IW-DOM (Table 3). Compounds consisting of C, H and O (CHO compounds) predominated in number and relative intensity in IW-DOM in all samples (Table 3). S- and N-bearing compounds (CHOS and CHNO compounds) had relative intensities below 30% in all samples except for the sample from 147 to 162 cm in which CHOS and CHNO compounds reached relative intensities of up to 42% and 35%, respectively. This sample also contained an elevated number of CHNOS compounds compared to the other IW-DOM samples (Table 3). In general, only few compounds contained P (CHOP compounds) or combinations of N and P or P and S.

The molecular composition of the IW-DOM changed with sediment depth. At 10–12 cm depth, the IW-DOM had a particularly elevated weighted average (wa) O/C ratio of 0.51 (Table 3) compared to O/C_{wa} values of 0.47 to 0.35 in the other samples. Although the variations in the weighted average values appear small, they were meaningful. The O/C_{wa} values in the duplicate analyses for the *E. coli* samples (duplicate extraction and analyses) differed only by 0.01 (Table 3). IW-DOM at 147–162 cm was characterized by an increased number and intensity of S-bearing compounds (S_{wa} of 0.40) and an elevated DBE_{wa} value of 8.55; i.e., molecular formulas contained a higher hydrogen deficiency (rings plus pi-bonds) compared to molecular formulas in the other IW-DOM samples. The IW-DOM sample from 420 to 435 cm showed the lowest O/C_{wa} ratio of 0.35 and an elevated H/C_{wa} ratio of 1.44 (Table 3). This is exemplified in the detailed mass spectrum on mass 385 in Fig. 1(a–d); molecular formulas with the highest peak intensities in sample 420–435 cm (Fig. 1c) are shifted to higher masses by 0.036 Da compared to the other samples, i.e., some of the O is replaced by CH_4 units which shifts the intensity weighted average values to lower O/C and higher H/C ratios. In 596–613 cm sediment depth, IW-DOM was characterized by the highest relative intensities of CHO-compounds.

Table 3
Numbers of identified formulas and peak magnitude weighted average values of molar oxygen-to-carbon (O/C_{wa}) and hydrogen-to-carbon ratios (H/C_{wa}), double bond equivalents (DBE_{wa}), elements (C_{wa}, S_{wa}, N_{wa}) and carbon-to-nitrogen ratio (N/C_{wa}) for the sum of all formulas in IW-DOM, WE-OM and *E. coli* extracts (two replicates).

	IW				WE					
	10–12 cm	147–162 cm	420–435 cm	596–613 cm	10–12 cm	147–167 cm	420–435 cm	596–613 cm	*E. coli* 1	*E. coli* 2
n(formulas)	3465	5790	3244	3593	6424	9356	9749	8360	1067	941
CHO	1243	1421	1249	1487	1570	1963	1923	1961	137	133
CHNO	926	1724	1027	1306	2527	3459	4051	3550	477	431
CHOS	949	1503	790	652	1472	2085	1772	1456	104	92
CHNOS	271	951	158	127	683	1522	1563	1061	117	98
H/C_{wa}	1.22	1.22	1.44	1.33	1.35	1.32	1.32	1.29	1.57	1.56
O/C_{wa}	0.51	0.47	0.35	0.47	0.47	0.46	0.46	0.48	0.35	0.36
DBE_{wa}	8.22	8.55	6.40	7.31	7.58	7.81	7.52	7.70	6.58	6.56
C_{wa}	18.1	18.5	19.0	18.3	18.2	18.4	17.8	17.8	18.3	18.0
S_{wa}	0.26	0.40	0.18	0.13	0.28	0.35	0.26	0.21	0.22	0.21
N_{wa}	0.28	0.45	0.28	0.32	1.23	1.00	0.94	0.73	1.86	1.85
C/N_{wa}	64.1	41.0	67.7	57.2	14.9	18.4	18.8	24.3	9.8	9.8

3.3.2. Molecular composition of WE-OM and its differences to IW-DOM

Compared to IW-DOM the WE-OM samples contained higher numbers of formulas (up to 9749) in the mass range of 180–600 Da. CHNO compounds predominated in number followed by CHO, CHOS and CHNOS compounds (Table 3); in the upper two samples single CHNO and CHOS peaks reached the highest relative intensities. The compound diversity in WE-OM and the molecular variations in different sediment depths differed considerably from IW-DOM as exemplarily shown for the mass 385 in Fig. 1. All spectra showed a similar pattern at the other masses with a generally lower number of total peaks per mass for $m/z < 300$ and a slightly lower resolution at $m/z > 500$. Thus, two to three times larger numbers of formulas were identified in all WE-OM samples compared to the corresponding IW-DOM sample. At 10–12 cm depth the WE-DOM spectrum showed several CHNO compounds containing four N atoms (homologous series from $C_{15}H_{22}O_8N_4$ to $C_{18}H_{34}O_5N_4$ with homologous being defined as the functional relationship between molecular formulas that differ by a specific mass difference equivalent to a chemical building block, e.g., CH_2 (14.01565 Da), CH_4 replaced by O (0.036 Da); cf. Koch et al., 2007). These tetra-N-atomic compounds had high intensities in the upper two samples and decreased with increasing sediment depth, whereas mono- and di-N-atomic CHNO compounds became intensity-wise more important (Fig. 2a). The deeper two WE-OM samples were clearly dominated by CHO compounds. Two different homologous series of CHO compounds were detected in all of the samples on the mass 385 (Fig. 1). Members of one homologous series differ by one CH_4 which is replaced by one O. The more unsaturated series ($C_{18}H_{10}O_{10}$ to $C_{22}H_{26}O_6$ with DBE from 14 to 10) had in general lower relative intensities compared to the more saturated CHO series ($C_{15}H_{14}O_{12}$ to $C_{22}H_{42}O_5$ with DBE from 9 to 2). Consistent with the trends in DBE_{wa} (Table 3), the former series was most abundant at 147–167 cm depth in both IW-DOM and WE-OM (Fig. 1). Similar to IW-DOM, CHOS compounds showed the highest relative intensities in 147–162 cm depth. Molecular formulas containing two S atoms were more abundant in WE-OM (Fig. 2a). WE-OM from 420 to 435 cm (limnic horizon) showed an O/C_{wa} ratio of 0.46, which is in the range of the other WE-OM samples and contrasted the corresponding IW-DOM sample from this depth (Table 3 and Section 3.3.1).

For an overview of the gain (and loss) of formulas with the different extraction methods differential mass spectra were calculated (Fig. 2b). The majority of molecular formulas present in both pools had higher relative intensities in WE-OM. Particularly CHNO compounds were enriched in WE-OM relative to IW-DOM. Only CHO formulas showed a distinct relative peak intensity loss in WE-OM compared to IW-DOM (Fig. 2); these compounds corresponded to the molecular formulas with low O/C ratios described above.

WE-OM contained a higher number of molecular formulas and unique compounds that were not observed in IW-DOM. Van Krevelen diagrams in Fig. 3 compare IW-DOM specific (black) to WE-OM specific (red) molecular formulas with respect to their elemental O/C and H/C ratios (a van Krevelen diagram showing 7460 formulas that are shared by at least one WE-OM and one IW-DOM sample is provided as Fig. S1 in Appendix A). Each symbol in the van Krevelen diagram represents one or more formulas with defined O/C and H/C ratios. Different organic compound classes have different O/C and H/C ratios and based on this, van Krevelen diagrams have been used to identify sources and transformation patterns in DOM (e.g., Kim et al., 2003; Sleighter and Hatcher, 2008; Schmidt et al., 2011). As expected, WE-OM showed a higher number of unique formulas for all compound groups compared to IW-DOM that were distributed over a wide H/C and O/C range (Fig. 3a). Specific CHO and CHOS compounds in IW-DOM had mostly low O/C ratios (<0.3), and variable H/C ratios (0.3–1.2). Some formulas plot at high O/C ratios and intermediate H/C ratios, while a second cluster plots at low H/C ratios and intermediate O/C ratios. Specific di-S-atomic CHOS compounds are less abundant; while they

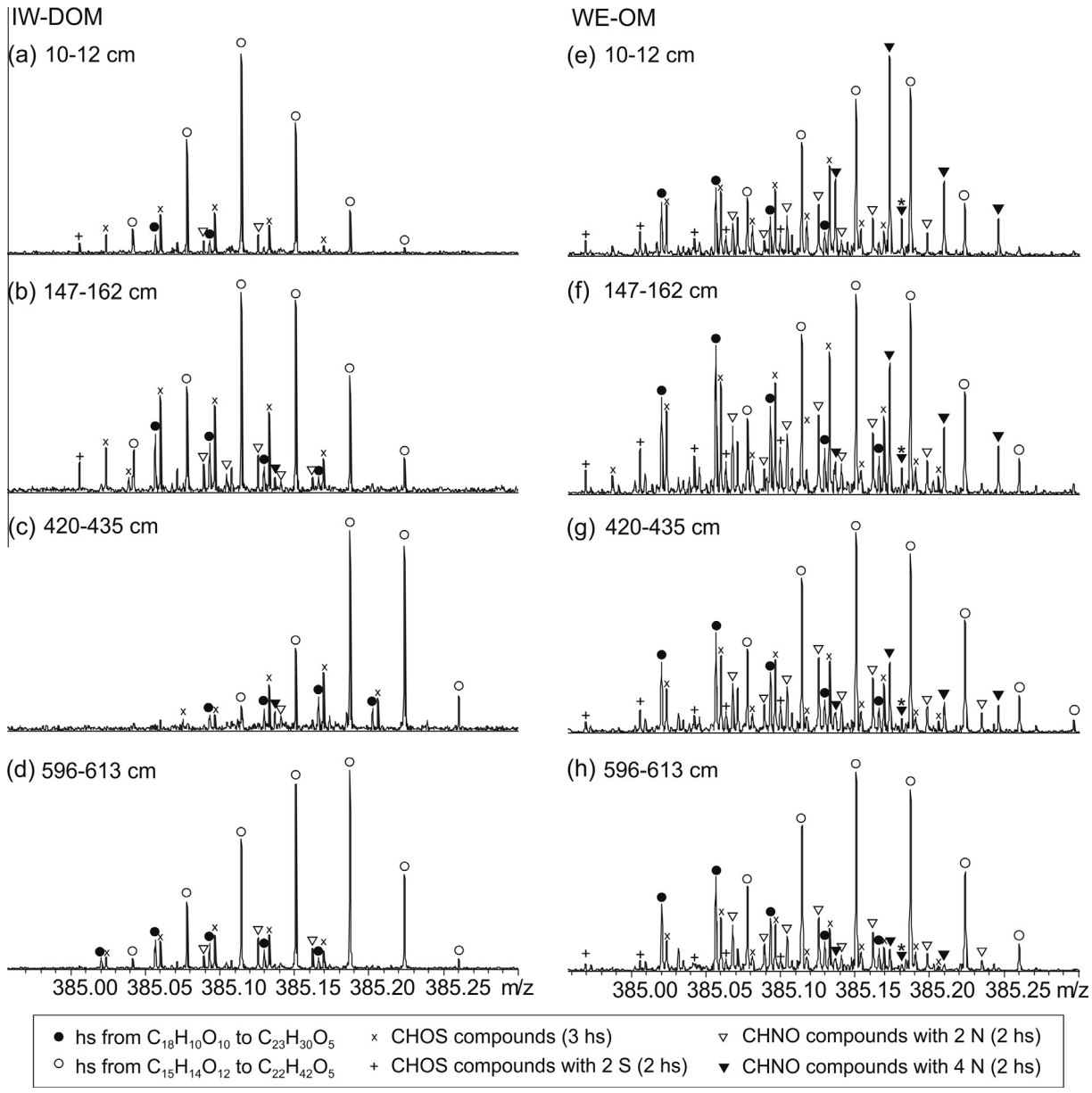

Fig. 1. FT-ICR mass spectra on the mass 385 Da for IW-DOM (left) and WE-OM (right) with increasing sediment depth from 10–12 cm (a and e), 147–162 cm (b and f), 420–435 cm (c and g), 596–613 cm (d and h). Symbols refer to different homologous series (hs). Triangle with star indicates the molecular formula $C_{17}H_{27}N_3O_7$ containing one ^{13}C; the corresponding parent ion ($^{12}C_{17}H_{27}N_3O_7$) is in a spacing of −1.00333 Da and is 5.4-times more abundant.

had low to intermediate O/C and H/C ratios in IW-DOM, specific WE-OM compounds had high O/C and H/C ratios (Fig. 3a). Specific CHNO compounds in WE-OM were highly abundant (relative intensities of up to 100% in 10–12 cm depth) and distributed over a wide O/C and H/C range except for tetra-N-atomic CHNO compounds, which mainly had elevated H/C ratios (Fig. 3b). IW-DOM-specific tri- and tetra-N-atomic CHNO compounds were less abundant (relative intensity < 6.5%) and plotted mainly in the center of the van Krevelen diagram where carboxyl-rich alicyclic molecules (CRAM) have been detected (Hertkorn et al., 2006). IW-specific mono- and di-N-atomic CHNO compounds were mainly detected at low O/C ratios and varying H/C ratios.

We performed a principle component analysis (PCA) to identify the molecular formulas that account for most of the variance in the different sample types (Figs. S2 and S3 in Appendix A). Principal component (PC) 1 and PC 2 explained together 72.8% of the variance. PC 1 separates IW-DOM from the three deeper WE-OM samples; mainly CHO, and CHNO compounds with intermediate O/C and a wide range of H/C values are associated with WE-OM, whereas CHO and CHNO compounds with mostly low O/C ratios are associated with IW-DOM as already

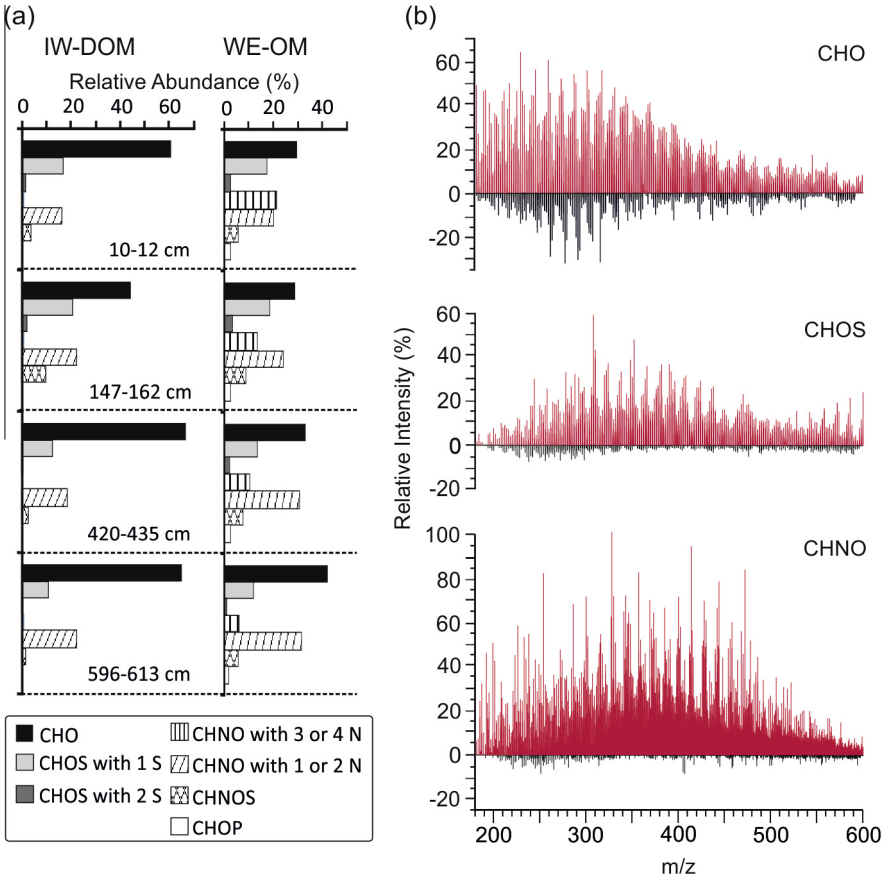

Fig. 2. (a) Relative abundance of different compound groups in IW-DOM (left panel) and WE-OM (right panel) for the different sediment depth of core GeoB 15105. (b) Differential FT-ICR mass spectra ($\sum$ peak intensities of all WE-OM samples minus $\sum$ peak intensities of all IW-DOM samples) showing peaks with a higher relative intensity in the WE-OM in red (positive) and peaks with a higher relative intensity in the IW-DOM in black (negative) for the three most abundant compound groups (CHO, CHOS, and CHNO). (For interpretation of the references to colour in this figure legend, the reader is referred to the web version of this article.)

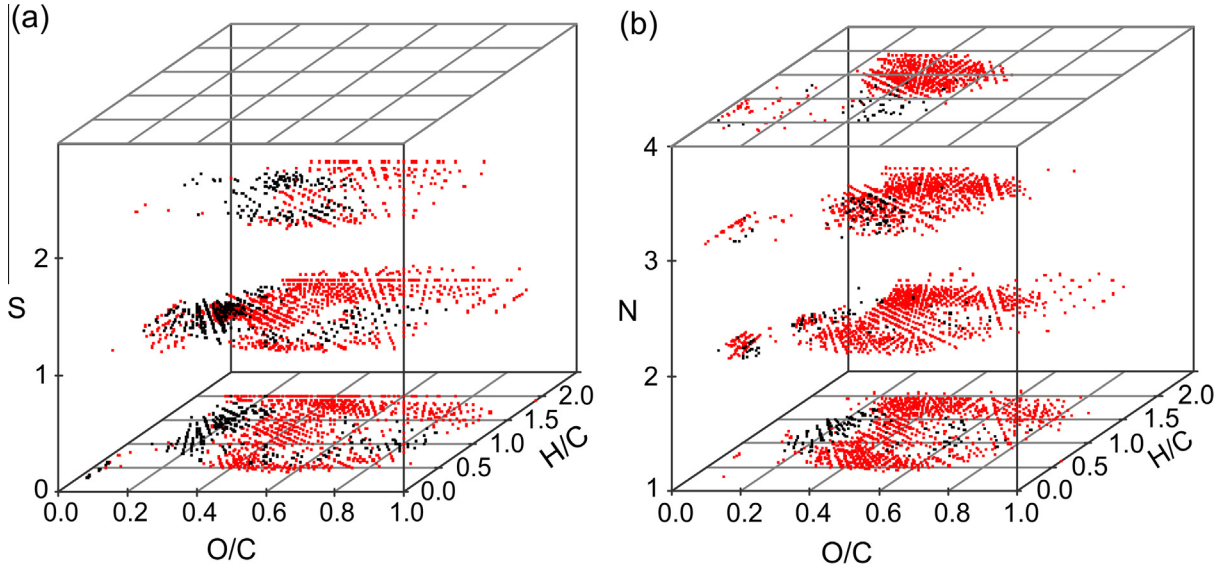

Fig. 3. Comparison of formulas between the WE-OM and the IW-DOM for (a) CHO and CHOS compounds, and (b) CHNO compounds. Formulas only present in the IW-DOM are shown in black and formulas only present in the WE-OM are displayed in red. (For interpretation of the references to colour in this figure legend, the reader is referred to the web version of this article.)

identified in Fig. 3. PC 2 describes the molecular variations in WE-OM with sediment depth where the upper two samples are characterized by tri- and tetra-N-atomic formulas with low to intermediate O/C and high H/C ratios and the deeper two by CHO compounds with CRAM composition as identified before by the increase in CHO compounds with depth (Figs. 1 and 2a).

3.4. *E. coli*

The Soxhlet extraction of *E. coli* cells yielded an average DOC concentration of 1040 μM and an average TDN concentration of 297 μM (Table 2). Extraction efficiencies were in the range of 56–58% and SPE-DON was comparably low (55 μM on average). The FT-ICR MS spectra of the *E. coli* samples contained around 1000 molecular formulas with a relative intensity > 3%. The duplicates showed only little variation, suggestive of a small analytical error. The O/C_{wa} ratio of 0.35 was low and the H/C_{wa} ratio of 1.57 elevated (Table 3). Molecular formulas containing S, N and/or P predominated in number and abundance, in particular CHNO compounds. This was indicated by very low C/N_{wa} ratios of around 10 compared to values of 15–24 for WE-OM and 41–64 for IW-DOM (Table 3).

4. DISCUSSION

4.1. Size of pools of IW-DOM and WE-OM and their amenability to molecular analyses

Aqueous Soxhlet extraction accessed considerable amounts of soluble organic carbon that represented up to 4.35% of the sedimentary TOC pool. Normalized to the sediment, DOC in WE-OM is 27 to 54 times larger than in the corresponding IW-DOM pool (Table 2). Thus, Soxhlet extraction yields a substantially larger number of potentially bioavailable organic compounds. On the other hand, this approach is limited by lower extraction efficiencies for Soxhlet extracts on PPL cartridges and thus larger fractions of organic matter that escape detection. DOC concentration in Soxhlet extracts was high enough for a direct injection without pre-concentration; however, the SPE step is a prerequisite to remove salts that would interfere with DOM molecules during electrospray ionization. The applied PPL cartridges are suited for polar compounds and work well for DOM in the marine water column and interstitial water. Extraction efficiencies of SPE on PPL cartridges range between 43% and 65% for marine water column DOM (Dittmar et al., 2008), and between 38% and 55% for IW-DOM from subsurface sediment (Schmidt et al., 2009, 2011) and yielded a maximum value of 87% for the sample from 596 to 613 cm in this study. Low $\delta^{13}C$ values in the lacustrine sediment (420–435 and 596–613 cm) indicated variations in organic matter composition that appeared to have a strong effect on the extraction efficiency. IW-DOM appeared to become less polar and hydrophilic with sediment depth and thus was more efficiently extracted with SPE. With the Soxhlet approach, we extracted either a fraction of highly hydrophilic compounds that were not retained on PPL resin or the PPL cartridges were overloaded and retaining capacities were exceeded. To exclude the latter, different volumes of the Soxhlet extracts (5, 10, 25 and 150 ml) were extracted on PPL cartridges but uniformly low extraction efficiencies of 15% were observed for all volumes (Table S3, Appendix A). Consequently, it appears that the lost DOC fraction was not retained on the cartridges due to its extreme hydrophilic properties.

4.2. Effect of geochemical conditions and burial depth on DOM composition

DOM in marine sediments is mainly released by depolymerization of buried particulate organic matter (Burdige et al., 2004). It is in exchange with the solid phase via dissolution and flocculation and therefore affected by the prevailing geochemical conditions such as pH, temperature, and ionic strength of the aqueous phase. The age of the sedimentary organic matter and burial depth influence its reactivity (Middelburg, 1989; Komada et al., 2013) and therefore influence the amount and composition of DOM. In the Black Sea, the sedimentary DOM composition was strongly controlled by the geochemical conditions. The increased abundance of the CHOS compounds (in number and intensity) at 147–162 cm depth in both IW-DOM and WE-OM probably resulted from sulfurization reactions caused by elevated interstitial water sulfide concentrations (4.4 mM HS^- compared to 1.7 mM and 0.3 mM in 10–12 cm and 420–435 cm depth, respectively; personal communication; T. Goldhammer and M. Zabel). Accumulation of CHOS compounds in DOM of rapidly accumulating mid-shelf mud has been demonstrated before (Schmidt et al., 2009) and probably results from reactions of functionalized molecules such as lipids and carbohydrates with free bisulfides, hydrogen sulfides or polysulfides, which bind to C–C double bonds by nucleophilic addition (Vairavamurthy and Mopper, 1987; Kohnen et al., 1989; Van Dongen et al., 2003). While unequivocal precursor-product relationships cannot be established without detailed structural information, potential genetic relationships between compounds can be explored on the basis of relationships of molecular formulas as well as the geochemical context. For example, one possible sulfurization reaction is the exchange of one O atom by one S atom and two H atoms during reduction. Using the detected CHO compound $C_{12}H_{14}O_7$ as an example (Table 4), we observe the putative reactant and its mono-S- and di-S-atomic products $C_{12}H_{16}O_6S_1$ and $C_{12}H_{18}O_5S_2$ in all samples. Sulfurization of a given set of formulas is substantially higher in the sulfide-rich horizon resulting in a strong increase in the S-bearing products compared to their putative precursors (Table 4).

Compared to the other sediment depths, IW-DOM constituents in 420–435 cm were shifted to lower O/C ratios (Fig. 1). The high relative abundance of these molecular formulas might be a result of specific geochemical conditions and could arise from (i) transformation reactions of DOM compounds in the interstitial water, (ii) the loss of carboxyl moieties, or (iii) the dissolution of a group of compounds with low O-content from particulate organic matter. The fact that this shift to lower O/C ratios was not

Table 4
Potential reactants and products of a sulfurization reaction (O replaced by H_2S) for the six most abundant mono-S-atomic CHOS formulas in (a) the IW-DOM sample and (b) the WE-OM sample from 147 to 162 cm depth in comparison to the corresponding sample from 10 to 12 cm depth. The sulfurization ratio was calculated for single molecular series and emphasizes the elevated abundance of CHOS compounds in the sulfide-rich horizon (147–162 cm depth).

Molecular series of O replaced by H_2S	Sulfurization ratio* [(CHO-S_1 + CHO-S_2)/CHO]	
	10–12 cm	147–162 cm
(a) IW-DOM		
$C_{12}H_{14}O_7$–$C_{12}H_{16}O_6S_1$–$C_{12}H_{18}O_5S_2$	0.83	1.60
$C_{13}H_{16}O_7$–$C_{13}H_{18}O_6S_1$–$C_{13}H_{20}O_5S_2$	0.45	0.82
$C_{14}H_{16}O_8$–$C_{14}H_{18}O_7S_1$–$C_{14}H_{20}O_6S_2$	0.48	1.00
$C_{13}H_{16}O_8$–$C_{13}H_{18}O_7S_1$–$C_{13}H_{20}O_6S_2$	0.44	0.81
$C_{12}H_{16}O_7$–$C_{12}H_{18}O_6S_1$–$C_{12}H_{20}O_5S_2$	0.40	0.66
$C_{12}H_{14}O_8$–$C_{12}H_{16}O_7S_1$–$C_{12}H_{18}O_6S_2$	0.89	1.68
(b) WE-DOM		
$C_{14}H_{28}O_6$–$C_{14}H_{30}O_5S_1$	0.70	9.98
$C_{13}H_{16}O_6$–$C_{13}H_{18}O_5S_1$–$C_{13}H_{20}O_4S_2$	0.95	1.53
$C_{18}H_{36}O_8$–$C_{18}H_{38}O_7S_1$	0.56	7.85
$C_{17}H_{26}O_4$–$C_{17}H_{28}O_3S_1$	0.97	5.03
$C_{15}H_{22}O_8$–$C_{15}H_{24}O_7S_1$	0.70	0.82
$C_{16}H_{28}O_7$–$C_{16}H_{30}O_6S_1$	0.82	1.32

* Calculated from the absolute peak magnitudes in MS.

observed in the WE-OM suggests that this process occurred in the interstitial water and that most of the WE-OM constituents were protected and not subjected to these molecular transformations. DOM adsorption is controlled by the mineralogy of sediment particles and the chemical properties of particulate organic matter. Montmorillonite (smectite group) adsorbs hydrophillic compounds such as amides, carbohydrates and alcohols, whereas kaolinite preferentially adsorbs polycyclic aromatic hydrocarbons (Zhang et al., 2009; Conte et al., 2011). At our site in the Black Sea the clay mineral composition changes from illite (Unit 1) over kaolinite and illite (Unit 2 and 3) to smectite (in 596–613 cm depth, Unit 3) (Major et al., 2002), and thus from hydrophobic to hydrophilic adsorbents. A release of relatively hydrophilic compounds from the deeper sediment during Soxhlet extraction could explain the decrease in extraction efficiencies of WE-OM with depth, because these compounds are less amenable to SPE. In general, WE-OM-specific formulas had higher O/C ratios (Fig. 3) and were thus enriched in carboxylic and hydroxylic groups with hydrophilic properties.

The high relative abundance of CHO compounds in all samples suggests that they are either permanently produced in the sediment or are recalcitrant molecules that accumulated in the interstitial water. An increase of these compounds with sediment depth in both IW-DOM and WE-OM is consistent with their accumulation due to the generally assumed increase in refractory compounds with on-going diagenesis (Middelburg, 1989; Burdige, 1991; Komada et al., 2013) and their predominance in aged deep ocean water DOM (Koch et al., 2005; Hertkorn et al., 2006; Lechtenfeld et al., 2014).

4.3. Characteristic organic matter fraction in WE-OM

A new compound pool was accessed via Soxhlet extraction. IW-DOM contained tri- and tetra-N-atomic CHNO compounds only in small amounts (0.2–1.1% relative abundance), while mono- and di-N-atomic CHNO compounds predominated (Fig. 2a). In WE-OM on the other hand, tri- and tetra-N-atomic CHNO compounds were remarkably abundant and in 10–12 cm sediment depth they were even slightly more abundant than the mono- and di-N-atomic CHNO compounds. A large fraction of tri- and tetra-N-atomic CHNO compounds with high H/C and low to intermediate O/C ratios (Fig. 3b) was also present in *E. coli* extracts (Fig. 4). 48% of the formulas shared by *E. coli* and WE-OM were tri- and tetra-N-atomic CHNO compounds. Most of these molecular formulas resembled

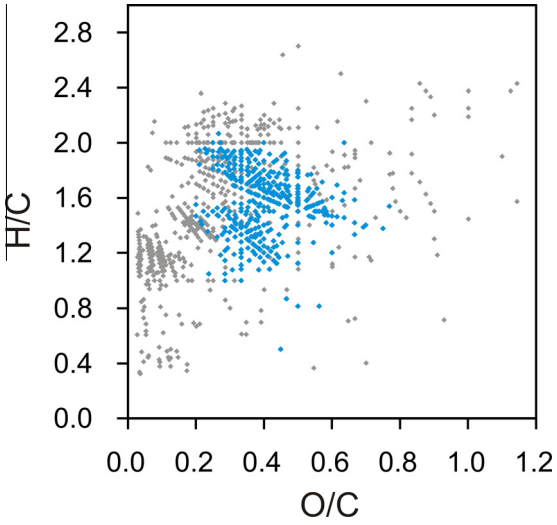

Fig. 4. Van Krevelen diagram of all 900 formulas detected in both *E. coli* samples. The subset of formulas shown in blue ($n = 558$) was also detected in WE-OM; 74% of these formulas contained N and 48% were tri and tetra-N-atomic formulas. (For interpretation of the references to colour in this figure legend, the reader is referred to the web version of this article.)

Table 5
Estimate of total protein contribution to sedimentary water-extractable TDN and DOC for typical cell abundances in the sediments from the Black Sea (Jørgensen, 2012). An average cell size of 500 nm corresponds to a cell dry mass of 34.4 fg (Simon and Azam, 1989).

Depth (cm)	Cell counts (cm^3)	Total protein dry mass ($\mu g/cm^3$)*	Total cell C dry mass ($\mu g/cm^3$)**	Total protein DON ($\mu g/cm^3$)	Proteins/ sed.TDN (%)	Cell C/sed DOC (%)
10–12	1E+09	21.67	18.58	3.47	8.78	3.94
147–162	1E+09	21.67	18.58	3.47	12.86	3.27
420–435	1E+08	2.17	1.86	0.35	1.45	0.36
596–613	1E+07	0.22	0.19	0.03	0.31	0.04

* 63% of cell dry mass.
** 54% of cell dry mass.

exact formulas of various tri- and tetra-peptides. For example, the highest peak in Fig. 1e, $C_{16}H_{26}O_7N_4$, could represent the tetrapeptides "serylprolylprolylserine" or "glutamylalanylalanylproline". Although our analyses yielded only exact masses and no structural information, it appears that peptides contributed to the DON in the Soxhlet extract from the uppermost sample. In contrast to tri- and tetra-N-atomic CHNO compounds, mono- and di-N-atomic CHNO compounds, i.e., molecules with one or two amide groups, were mostly too large to be amino acids (<204 Da) or dipeptides (<342 Da). It has been suggested that these compounds derive from proteins and peptides that have been altered by biotic and abiotic early-diagenetic reactions such as deamination, oxidation, and hydration (Schmidt et al., 2011).

The peptide-like formulas in WE-OM may partly be derived from destruction of microbial cells during Soxhlet extraction. In soils hot water extracted C correlates significantly with microbial biomass C (Sparling et al., 1998; Ghani et al., 2003). Around 60% of the dry mass of microbial cells consists of proteins (Simon and Azam, 1989). The release of cellular proteins during extraction might result from deionized water that destroyed intact cells by osmotic pressure. This process possibly was accompanied by hydrolysis of proteins to smaller peptides. We estimated the potential maximum effect caused by protein degradation during extraction due to cell destruction (Table 5) by assuming an abundance of 10^9 cells per mL in the upper sediment and 10^7 cells per mL at 6 m depth as it has been reported for the Black Sea (Jørgensen, 2012). With an average cell diameter of 500 nm and a cell dry mass of 34.4 fg, we estimated 21.7 fg proteins per cell (63% of cell dry mass) and cell carbon content of 18.6 fg (54% of the cell dry mass) (Simon and Azam, 1989). Accordingly, for the unlikely event that all proteinaceous components were turned into water-soluble compounds, the contribution of cellular components could amount up to 8.8% of TDN and 3.9% of DOC derived from proteins in the 10–12 cm sample and 0.31% of TDN and 0.04% of DOC in the 596–613 cm horizon (Table 5). Therefore the effect of cell lysis in the deeper samples examined in this study is likely negligible. To further elucidate the effect of Soxhlet extraction on microbial cells and to quantify the amount of N that is released from the destruction of cells, we subjected *E. coli* to aqueous Soxhlet extraction. Our results show that on average 24.2% of the total proteinaceous N and 11.8% of the total cellular C is in the dissolved fraction <0.4 μm after Soxhlet extraction (Table S4 Appendix A). We therefore conclude that the release of peptides and other organic compounds from intact microbial cells could potentially yield peptide-like formulas. The expected effects of cell destruction are small (<0.5% of DOC and <2.1% of TDN) and are not consistent with the gradual trends observed in the down-core distribution of tri- and tetra-N-atomic CHNO compounds (Fig. 2a), whose relative abundance decreased from 21.4% over 13.4% and 10.5% to 6.0%. Consequently, the high abundance of CHNO compounds in WE-OM and the changing ratios of tri- and tetra-N-atomic vs. mono- and di-N-atomic compounds with depth likely represent the progressive early diagenetic degradation of sedimentary proteins with depth. However, structural analyses of these compounds will be needed to confirm their proteinaceous nature. The absence of peptide formulas in IW-DOM suggests that these compounds are immediately consumed by benthic microbes after dissolution.

5. CONCLUSIONS

Aqueous Soxhlet extraction of sediments provides access to a larger and more diverse DOM pool than conventional interstitial water sampling methods such as Rhizon sampling. DOM in the Soxhlet extracts was apparently highly hydrophilic and therefore the yields of subsequent DOM isolation using solid-phase extraction cartridges were comparatively low. Future studies using Soxhlet extraction should consider isolation protocols such as coupled reverse osmosis–electrodialysis (Koprivnjak et al., 2009) aiming at these extremely hydrophilic compounds. Increased temperatures of approximately 80 °C during Soxhlet extraction did not notably alter the DOM distribution of the interstitial water since the majority of IW-DOM compounds were also detectable in WE-OM. Compared to the IW-DOM pool, the WE-OM pool appeared to consist of fresher, less degraded constituents and therefore WE-OM provides a more comprehensive picture of the organic matter in the sediment. Moreover, aqueous Soxhlet extraction is a promising alternative to interstitial water analyses for deeply buried sediment, when FT-ICR MS analyses of interstitial waters are impossible due to limited sample availability.

ACKNOWLEDGEMENTS

We thank the crew, chief scientist Matthias Zabel, and the scientific shipboard party of the RV Meteor cruise M84-1

(DARCSEAS). We are grateful to Philippe Schmitt-Kopplin, Mourad Harir and Ivan Dubinenkov for FT-ICR MS measurements of *E. coli* extracts. Jenny Wendt is acknowledged for TOC and TN measurements. We thank Martin Könneke for providing *E. coli* and Felix Elling for cell counts. Gunnar Schmidt is thanked for support on the FT-ICR MS data evaluation by providing a *PHYTHON* script. We thank Marc Norman and the associate editor Thomas Bianchi for handling the manuscript and four anonymous reviewers for their constructive comments. Funding was provided by the European Research Council under the European Union's Seventh Framework Programme–"Ideas" Specific Programme, ERC grant agreement No. 247153 to KUH.

APPENDIX A. SUPPLEMENTARY DATA

Supplementary data associated with this article can be found, in the online version, at http://dx.doi.org/10.1016/j.gca.2014.06.009.

REFERENCES

Arnarson T. S. and Keil R. G. (2005) Influence of organic-mineral aggregates on microbial degradation of the dinoflagellate *Scrippsiella trochoidea*. *Geochim. Cosmochim. Acta* **69**, 2111–2117.

Arnosti C., Steen A. D., Ziervogel K., Ghobrial S. and Jeffrey W. H. (2011) Latitudinal gradients in degradation of marine dissolved organic carbon. *PLoS One* **6**, e28900.

Bahr A., Arz H. W., Lamy F. and Wefer G. (2006) Late glacial to Holocene paleoenvironmental evolution of the Black Sea, reconstructed with stable oxygen isotope records obtained on ostracod shells. *Earth Planet. Sci. Lett.* **241**, 863–875.

Bhatia M. P., Das S. B., Longnecker K., Charette M. A. and Kujawinski E. B. (2010) Molecular characterization of dissolved organic matter associated with the Greenland ice sheet. *Geochim. Cosmochim. Acta* **74**, 3768–3784.

Biddle J. F., Lipp J. S., Lever M. A., Lloyd K. G., Sørensen K. B., Anderson R., Fredricks H. F., Elvert M., Kelly T. J., Schrag D. P., Sogin M. L., Brenchley J. E., Teske A., House C. H. and Hinrichs K.-U. (2006) Heterotrophic Archaea dominate sedimentary subsurface ecosystems off Peru. *Proc. Natl. Acad. Sci. U.S.A.* **103**, 3846–3851.

Bu X., Wang L., Ma W., Yu X., McDowell W. H. and Ruan H. (2010) Spectroscopic characterization of hot-water extractable organic matter from soils under four different vegetation types along an elevation gradient in the Wuyi Mountains. *Geoderma* **159**, 139–146.

Burdige D. J. (1991) The kinetics of organic matter mineralization in anoxic marine sediments. *J. Mar. Res.* **49**, 727–761.

Burdige D. J., Kline S. W. and Chen W. (2004) Fluorescent dissolved organic matter in marine sediment pore waters. *Mar. Chem.* **89**, 289–311.

Conte P., Abbate C., Baglieri A., Nègre M., Pasquale C. D., Alonzo G. and Gennari M. (2011) Adsorption of dissolved organic matter on clay minerals as assessed by infra-red, CPMAS 13C NMR spectroscopy and low field T1 NMR relaxometry. *Org. Geochem.* **42**, 972–977.

Curtin D., Beare M. H., Chantigny M. H. and Greenfield L. G. (2011) Controls on the extractability of soil organic matter in water over the 20 to 80 °C temperature range. *Soil Sci. Soc. Am. J.* **75**, 1423–1430.

D'Andrilli J., Chanton J. P., Glaser P. H. and Cooper W. T. (2010) Characterization of dissolved organic matter in northern peatland soil porewaters by ultra high resolution mass spectrometry. *Org. Geochem.* **41**, 791–799.

Degens E. T. and Ross D. A. (1972) Chronology of the Black Sea over the last 25,000 years. *Chem. Geol.* **10**, 1–16.

D'Hondt S., Rutherford S. and Spivack A. J. (2002) Metabolic activity of subsurface life in deep-sea sediments. *Science* **295**, 2067–2070.

D'Hondt S., Jørgensen B. B., Miller D. J., Batzke A., Blake R., Cragg B. A., Cypionka H., Dickens G. R., Ferdelman T., Hinrichs K.-U., Holm N. G., Mitterer R., Spivack A., Wang G., Bekins B., Engelen B., Ford K., Gettemy G., Rutherford S. D., Sass H., Skilbeck C. G., Aiello I. W., Guèrin G., House C. H., Inagaki F., Meister P., Naehr T., Niitsuma S., Parkes R. J., Schippers A., Smith D. C., Teske A., Wiegel J., Padilla C. N. and Acosta J. L. S. (2004) Distributions of microbial activities in deep subseafloor sediments. *Science* **306**, 2216–2221.

Dittmar T. and Koch B. P. (2006) Thermogenic organic matter dissolved in the abyssal ocean. *Mar. Chem.* **102**, 208–217.

Dittmar T., Koch B., Hertkorn N. and Kattner G. (2008) A simple and efficient method for the solid-phase extraction of dissolved organic matter (SPE-DOM) from seawater. *Limnol. Oceanogr. Methods* **6**, 230–235.

Friedrich W. L., Kromer B., Friedrich M., Heinemeier J., Pfeiffer T. and Talamo S. (2006) Santorini eruption radiocarbon dated to 1627–1600 B.C. *Science* **312**, 548.

Ghani A., Dexter M. and Perrott K. W. (2003) Hot-water extractable carbon in soils: a sensitive measurement for determining impacts of fertilisation, grazing and cultivation. *Soil Biol. Biochem.* **35**, 1231–1243.

Gonsior M., Peake B. M., Cooper W. T., Podgorski D., D'Andrilli J. and Cooper W. J. (2009) Photochemically induced changes in dissolved organic matter identified by ultrahigh resolution Fourier transform ion cyclotron resonance mass spectrometry. *Environ. Sci. Technol.* **43**, 698–703.

Gregorich E. G., Beare M. H., Stoklas U. and St-Georges P. (2003) Biodegradability of soluble organic matter in maize-cropped soils. *Geoderma* **113**, 237–252.

Grinhut T., Hertkorn N., Schmitt-Kopplin P., Hadar Y. and Chen Y. (2011) Mechanisms of humic acids degradation by white rot fungi explored using 1H NMR spectroscopy and FTICR mass spectrometry. *Environ. Sci. Technol.* **45**, 2748–2754.

Hedges J. I. and Keil R. G. (1995) Sedimentary organic matter preservation: an assessment and speculative synthesis. *Mar. Chem.* **49**, 81–115.

Hertkorn N., Benner R., Frommberger M., Schmitt-Kopplin P., Witt M., Kaiser K., Kettrup A. and Hedges J. I. (2006) Characterization of a major refractory component of marine dissolved organic matter. *Geochim. Cosmochim. Acta* **70**, 2990–3010.

Hertkorn N., Frommberger M., Witt M., Koch B. P., Schmitt-Kopplin P. and Perdue E. M. (2008) Natural organic matter and the event horizon of mass spectrometry. *Anal. Chem.* **80**, 8908–8919.

Jørgensen B. B. (2012) Shrinking majority of the deep biosphere. *Proc. Natl. Acad. Sci. U.S.A.* **109**, 15976–15977.

Keil R. G., Montlucon D. B., Prahl F. G. and Hedges J. I. (1994) Sorptive preservation of labile organic matter in marine sediments. *Nature* **370**, 549–552.

Kido Soule M. C., Longnecker K., Giovannoni S. J. and Kujawinski E. B. (2010) Impact of instrument and experiment parameters on reproducibility of ultrahigh resolution ESI FT-ICR mass spectra of natural organic matter. *Org. Geochem.* **41**, 725–733.

Kim S., Kramer R. W. and Hatcher P. G. (2003) Graphical method for analysis of ultrahigh-resolution broadband mass spectra of

natural organic matter, the Van Krevelen diagram. *Anal. Chem.* **75**, 5336–5344.

Kim S., Kaplan L. A., Benner R. and Hatcher P. G. (2004) Hydrogen-deficient molecules in natural riverine water samples-evidence for the existence of black carbon in DOM. *Mar. Chem.* **92**, 225–234.

Kim S., Kaplan L. A. and Hatcher P. G. (2006) Biodegradable dissolved organic matter in a temperate and a tropical stream determined from ultra-high resolution mass spectrometry. *Limnol. Oceanogr.* **51**, 1054–1063.

Koch B. P., Witt M., Engbrodt R., Dittmar T. and Kattner G. (2005) Molecular formulae of marine and terrigenous dissolved organic matter detected by electrospray ionization Fourier transform ion cyclotron resonance mass spectrometry. *Geochim. Cosmochim. Acta* **69**, 3299–3308.

Koch B. P., Dittmar T., Witt M. and Kattner G. (2007) Fundamentals of molecular formula assignment to ultrahigh resolution mass data of natural organic matter. *Anal. Chem.* **79**, 1758–1763.

Kohnen M. E. L., Damste J. S. S., ten Haven H. L. and de Leeuw J. W. (1989) Early incorporation of polysulphides in sedimentary organic matter. *Nature* **341**, 640–641.

Komada T., Burdige D. J., Crispo S. M., Druffel E. R. M., Griffin S., Johnson L. and Le D. (2013) Dissolved organic carbon dynamics in anaerobic sediments of the Santa Monica Basin. *Geochim. Cosmochim. Acta* **110**, 253–273.

Koprivnjak J. F., Pfromm P. H., Ingall E., Vetter T. A., Schmitt-Kopplin P., Hertkorn N., Frommberger M., Knicker H. and Perdue E. M. (2009) Chemical and spectroscopic characterization of marine dissolved organic matter isolated using coupled reverse osmosis–electrodialysis. *Geochim. Cosmochim. Acta* **73**, 4215–4231.

Kujawinski E. B., Del Vecchio R., Blough N. V., Klein G. C. and Marshall A. G. (2004) Probing molecular-level transformations of dissolved organic matter: insights on photochemical degradation and protozoan modification of DOM from electrospray ionization Fourier transform ion cyclotron resonance mass spectrometry. *Mar. Chem.* **92**, 23–37.

Kvenvolden K. A. (1993) Gas hydrates-geological perspective and global change. *Rev. Geophys.* **31**, 173–187.

Kwiecien O. and Haug G. (2008) Estimated reservoir ages of the Black Sea since the last glacial. *Radiocarbon* **50**, 99–118.

Lechtenfeld O. J., Koch B. P., Gašparović B., Frka S., Witt M. and Kattner G. (2013) The influence of salinity on the molecular and optical properties of surface microlayers in a karstic estuary. *Mar. Chem.* **150**, 25–38.

Lechtenfeld O. J., Kattner G., Flerus R., Leigh McCallister S., Schmitt-Kopplin P. and Koch B. P. (2014) Molecular transformation and degradation of refractory dissolved organic matter in the Atlantic and Southern Ocean. *Geochim. Cosmochim. Acta* **126**, 312–337.

Longnecker K. and Kujawinski E. B. (2011) Composition of dissolved organic matter in groundwater. *Geochim. Cosmochim. Acta* **75**, 2752–2761.

Lunau M., Lemke A., Walther K., Martens-Habbena W. and Simon M. (2005) An improved method for counting bacteria from sediments and turbid environments by epifluorescence microscopy. *Environ. Microbiol.* **7**, 961–968.

Major C., Ryan W., Lericolais G. and Hajdas I. (2002) Constraints on Black Sea outflow to the Sea of Marmara during the last glacial–interglacial transition. *Mar. Geol.* **190**, 19–34.

Middelburg J. J. (1989) A simple rate model for organic matter decomposition in marine sediments. *Geochim. Cosmochim. Acta* **53**, 1577–1581.

Parkes R. J., Cragg B. A. and Wellsbury P. (2000) Recent studies on bacterial populations and processes in subseafloor sediments: a review. *Hydrogeol. J.* **8**, 11–28.

Reemtsma T., These A., Linscheid M., Leenheer J. and Spitzy A. (2008) Molecular and structural characterization of dissolved organic matter from the deep ocean by FTICR-MS, including hydrophilic nitrogenous organic molecules. *Environ. Sci. Technol.* **42**, 1430–1437.

Roth V.-N., Dittmar T., Gaupp R. and Gleixner G. (2013) Latitude and pH driven trends in the molecular composition of DOM across a north south transect along the Yenisei River. *Geochim. Cosmochim. Acta* **123**, 93–105.

Sarkhot D. V., Grunwald S., Ge Y. and Morgan C. L. S. (2011) Comparison and detection of total and available soil carbon fractions using visible/near infrared diffuse reflectance spectroscopy. *Geoderma* **164**, 22–32.

Schmidt F., Elvert M., Koch B. P., Witt M. and Hinrichs K.-U. (2009) Molecular characterization of dissolved organic matter in pore water of continental shelf sediments. *Geochim. Cosmochim. Acta* **73**, 3337–3358.

Schmidt F., Koch B. P., Elvert M., Schmidt G., Witt M. and Hinrichs K.-U. (2011) Diagenetic transformation of dissolved organic nitrogen compounds under contrasting sedimentary redox conditions in the Black Sea. *Environ. Sci. Technol.* **45**, 5223–5229.

Seeberg-Elverfeldt J., Schlüter M., Feseker T. and Kölling M. (2005) Rhizon sampling of pore waters near the sediment/water interface of aquatic systems. *Limnol. Oceanogr. Methods* **3**, 361–371.

Simon M. and Azam F. (1989) Protein content and protein synthesis rates of planktonic marine bacteria. *Mar. Ecol. Prog.* **51**, 201–213.

Sleighter R. L. and Hatcher P. G. (2008) Molecular characterization of dissolved organic matter (DOM) along a river to ocean transect of the lower Chesapeake Bay by ultrahigh resolution electrospray ionization Fourier transform ion cyclotron resonance mass spectrometry. *Mar. Chem.* **110**, 140–152.

Sleighter R. L., Chen H., Wozniak A. S., Willoughby A. S., Caricasole P. and Hatcher P. G. (2012) Establishing a measure of reproducibility of ultrahigh-resolution mass spectra for complex mixtures of natural organic matter. *Anal. Chem.* **84**, 9184–9191.

Sparling G., Vojvodić-Vuković M. and Schipper L. A. (1998) Hot-water-soluble C as a simple measure of labile soil organic matter: the relationship with microbial biomass C. *Soil Biol. Biochem.* **30**, 1469–1472.

Tremblay L. B., Dittmar T., Marshall A. G., Cooper W. J. and Cooper W. T. (2007) Molecular characterization of dissolved organic matter in a North Brazilian mangrove porewater and mangrove-fringed estuaries by ultrahigh resolution Fourier Transform-Ion Cyclotron Resonance mass spectrometry and excitation/emission spectroscopy. *Mar. Chem.* **105**, 15–29.

Vairavamurthy A. and Mopper K. (1987) Geochemical formation of organosulphur compounds (thiols) by addition of H2S to sedimentary organic matter. *Nature* **329**, 623–625.

van Dongen B. E., Schouten S., Baas M., Geenevasen J. A. J. and Sinninghe Damsté J. S. (2003) An experimental study of the low-temperature sulfurization of carbohydrates. *Org. Geochem.* **34**, 1129–1144.

Veuger B., van Oevelen D. and Middelburg J. J. (2012) Fate of microbial nitrogen, carbon, hydrolysable amino acids, monosaccharides, and fatty acids in sediment. *Geochim. Cosmochim. Acta* **83**, 217–233.

Vieth A., Mangelsdorf K., Sykes R. and Horsfield B. (2008) Water extraction of coals – potential for estimating low molecular

weight organic acids as carbon feedstock for the deep terrestrial biosphere. *Org. Geochem.* **39**, 985–991.

Wakeham S. G., Lee C., Hedges J. I., Hernes P. J. and Peterson M. J. (1997) Molecular indicators of diagenetic status in marine organic matter. *Geochim. Cosmochim. Acta* **61**, 5363–5369.

Webster G., John Parkes R., Cragg B. A., Newberry C. J., Weightman A. J. and Fry J. C. (2006) Prokaryotic community composition and biogeochemical processes in deep subseafloor sediments from the Peru Margin. *FEMS Microbiol. Ecol.* **58**, 65–85.

Weiss M., Abele U., Weckesser J., Welte W., Schiltz E. and Schulz G. (1991) Molecular architecture and electrostatic properties of a bacterial porin. *Science* **254**, 1627–1630.

Whitman W. B., Coleman D. C. and Wiebe W. J. (1998) Prokaryotes: the unseen majority. *Proc. Natl. Acad. Sci. U.S.A.* **95**, 6578–6583.

Xing S., Chen C., Zhou B., Zhang H., Nang Z. and Xu Z. (2010) Soil soluble organic nitrogen and active microbial characteristics under adjacent coniferous and broadleaf plantation forests. *J. Soils Sediments* **10**, 748–757.

Zhang X., Hong H., Li Z., Guan J. and Schulz L. (2009) Removal of azobenzene from water by kaolinite. *J. Hazard. Mater.* **170**, 1064–1069.

Associate editor: Thomas S. Bianchi